

The first-principle study of N₂O gas interaction on the surface of pristine and Si-, Ga-, SiGa-doped of armchair boron phosphide nanotube using DFT method

M Rezaei-Sameti and Kh Hadian

Department of Physical Chemistry, Faculty of Science, Malayer University, Malayer, Iran

E-mail: mrsameti@maleru.ac.ir

(Received 2 March 2016 ; in final form 18 July 2016)

Abstract

In present research, the electrical, structural, quantum and Nuclear Magnetic Resonance (NMR) parameters of interaction of N₂O gas on the B and P sites of pristine, Ga-, Si- and SiGa-doped (4,4) armchair models of boron phosphide nanotubes (BPNTs) are investigated by using density functional theory (DFT). For this purpose, seven models for adsorption of N₂O gas on the exterior surfaces of BPNTs have been considered and then all structures are optimized by B3LYP level of theory and 6-31G (d) base set. The optimized structures are used to calculate the electrical, structural, quantum and NMR parameters. The computational results revealed that the adsorption energy of all studied models of BPNTs is negative; all processes are exothermic and favorable in thermodynamic approach. When N₂O gas is adsorbed from its O atom head on the B site of nanotube, N₂O gas is dissociated to O atom and N₂ molecule. The adsorption energy of this process is more than those of other models and more stable than other models. In A, B and C models, the global hardness decreases significantly from original values and so the activity of nanotube increases from original state. On the other hand, the electrophilicity index (ω), electronic chemical potential (μ), electronegativity (χ) and global softness (S) of the A, B and C models increase significantly from original value and CSI values of the C model are larger than those of other models. The results demonstrate that the Ga-, Si- and SiGa- doped BPNTs are good candidates to adsorb N₂O and make N₂O gas sensor.

Keywords: BPNTs, DFT, NMR, N₂O adsorption, Ga-, Si- and SiGa-doped

1. Introduction

Nitrous oxide (N₂O) is a colorless, non-flammable gas, with a slightly sweet odour and taste. It is used in surgery and dentistry for its anaesthetic and analgesic effects [1]. N₂O has been generated as a byproduct in nitric and adipic acids [2–5]. Environmental researches show that N₂O gas is an environmental pollutant and a relatively strong greenhouse. It has an important role in destruction of ozone layer in stratosphere, for this reason, extensive researches are carried out to adsorb and control N₂O gas from stratosphere and environment by theoretical and experimental investigations [6–15]. Baei et al. [9–10] illustrate that adsorption energy for N₂O on the surface of (6, 0), (7, 0), and (8, 0) zigzag models of BNNTs in O-down is a little more than that in N-down. Inspection of the results of Soltani et al. [11] elucidates that with adsorbing N₂O gas on AlNNTs and AlPNTs, electronic properties of nanotubes would be changed, and adsorption of N₂O gas on the (6, 0) zigzag AlNNTs is more stable than (4, 4) armchair model. Boron phosphide nanotubes are inorganic analogs of

carbon nanotubes (CNTs) and have good physical properties for a broad variety of applications. In recent years, extensive research has been done on the structural, electrical, NMR and NQR parameters and adsorption of C₆H₆, H₂O₂, CO and NO on the surface of boron phosphide nanotube [12–20].

Following previous researches on the effects of Ga-, Ge-, Ge-As, Ga-As doped on electrical, structural and NMR parameters of armchair and zigzag models of BPNTs [21–25], in present project, adsorption energy, structural and electrical parameters of the nanotube/N₂O complex and the effects of Si-, Ga- and SiGa-doped on N₂O adsorption have been investigated on the surface of (4, 4) armchair boron phosphide nanotube (BPNTs). Structural, NMR, NBO and quantum parameters including HOMO, LOMU orbital, energy gap, electronic chemical potential (μ), global hardness (η), electrophilicity index (ω), energy gap ($\Delta E_{(gap)}$), global softness (S), and electronegativity (χ) have been determined for all adsorption models by using Gaussian 03 program package [26].

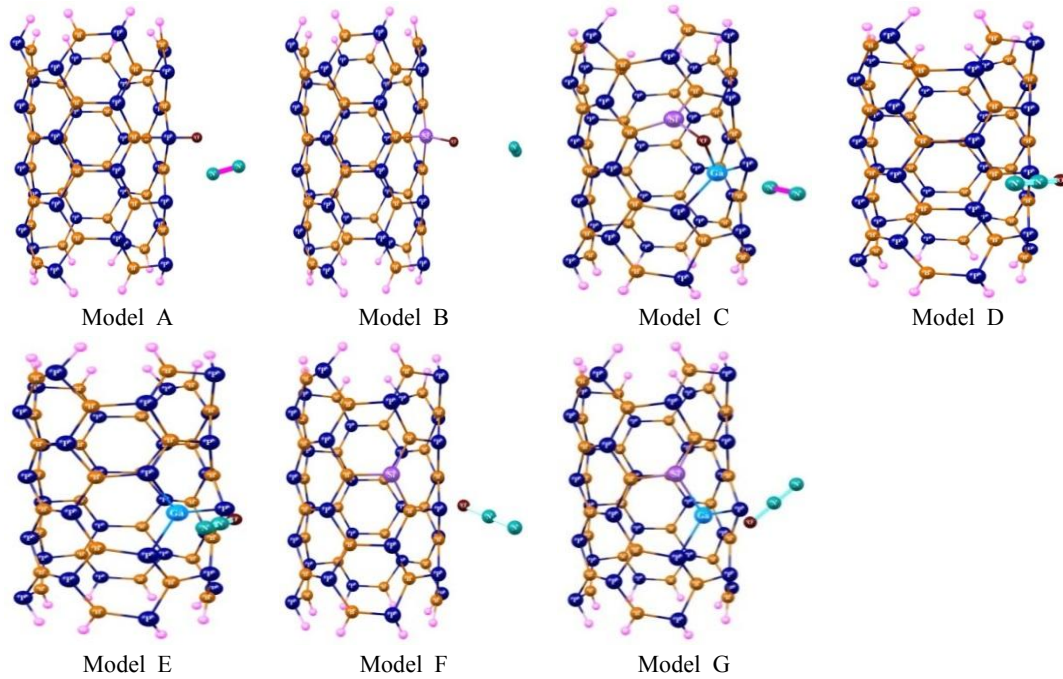


Figure 1. 2-D views of N₂O adsorption on the surface of (4, 4) armchair model BPNTs of (A–G) models.

2. Computational methods

In the first step, all adsorption structures are allowed to relax by all atomic geometrical optimization at B3LYP/6-31G (d) methods by using GAUSSIAN 03 program [26]. The optimized structures are used to determine adsorption energy, NMR, NBO, and quantum parameters of N₂O adsorption.

Adsorption energy (E_{ads}) of N₂O gas on the surface of BPNTs is calculated as follows:

$$E_{ads} = E_{BPNTs-N_2O} - (E_{BPNTs} + E_{N_2O}), \quad (1)$$

where $E_{BPNTs-N_2O}$, E_{BPNTs} , and E_{N_2O} energies are obtained from the optimized BPNTs/N₂O, BPNTs and N₂O gas respectively. Quantum molecular descriptors electronic Fermi level energy (E_{FL}), electronic chemical potential (μ), global hardness (η), electrophilicity index (ω), energy gap (E_{gap}), global softness (S), electronegativity (χ), and work function (ϕ) of the nanotubes are calculated as follows [21–25]:

$$\mu = -(I + A) / 2, \quad (2)$$

$$\eta = (I - A) / 2, \quad (3)$$

$$\chi = -\mu, \quad (4)$$

$$\omega = \mu^2 / 2\eta, \quad (5)$$

$$S = 1 / 2\eta, \quad (6)$$

$$E_{FL} = (E_{HOMO} + E_{LUMO}) / 2, \quad (7)$$

$$\phi = E_{HOMO} - E_{FL}, \quad (8)$$

$$E_{gap} = E_{LUMO} - E_{HOMO}, \quad (9)$$

where I ($-E_{HOMO}$) is the ionization potential and A ($-E_{LUMO}$) the electron affinity of the molecule.

Chemical shielding (CS) tensors at the sites of ¹¹B, ³¹P nuclei are calculated in the principal axes system (PAS) ($\sigma_{33} > \sigma_{22} > \sigma_{11}$) and are converted to measurable NMR parameters, Chemical Shielding Isotropic (CSI) and Chemical Shielding Anisotropic

(CSA) by using eqs. (10) and (11), respectively [21–25].

$$CSI(ppm) = \frac{1}{3}(\sigma_{11} + \sigma_{22} + \sigma_{33}), \quad (10)$$

$$CSA(ppm) = \sigma_{33} - (\sigma_{22} + \sigma_{33}) / 2. \quad (11)$$

3. Results and discussion

3.1 Optimized geometry parameters

In order to identify the most stable configuration, several potential configurations have been considered, including N₂O molecule is initially placed above pristine, Si-, Ga-, and SiGa-doped BPNTs. After structural optimizations, re-orientation of the molecule has been predicted in some configurations, and finally, stable configurations are obtained. Stable configurations for adsorption N₂O gas are renamed as A, B, C, D, E, F, and G models:

Adsorption of N₂O gas on the P41 site of pristine (A model), on the P41/Si site of Si-doped (B model), on the P41/Si site of GaSi-doped (C model), on the B51 site of pristine (D model), on the B51/Ga site of Ga-doped (E model), on the B51 site of Si-doped (F model), on the B51/Ga site of GaSi-doped (G model), BPNTs via oxygen head and in which the ends of the nanotubes are saturated by hydrogen atoms. The final optimized geometry of the N₂O/BPNTs complexes is depicted in figure 1.

From optimized structures of A–G models (Figure 1), geometrics parameters, including bond length (B–P) and bond angle (B–P–B) of neighbor adsorption and doping positions are determined and the results are given in Appendix (table 1) and shown in figure 2. Geometrical results show that the average bond length (B–P) and bond angle (B–P–B) of pristine BPNTs are 1.89 Å and 121.40° respectively, which are in agreement with previous results reported by other researchers[17–20, 26–29]. With doping Si on P41 nuclei, the bond length and bond angle of around doping position changes

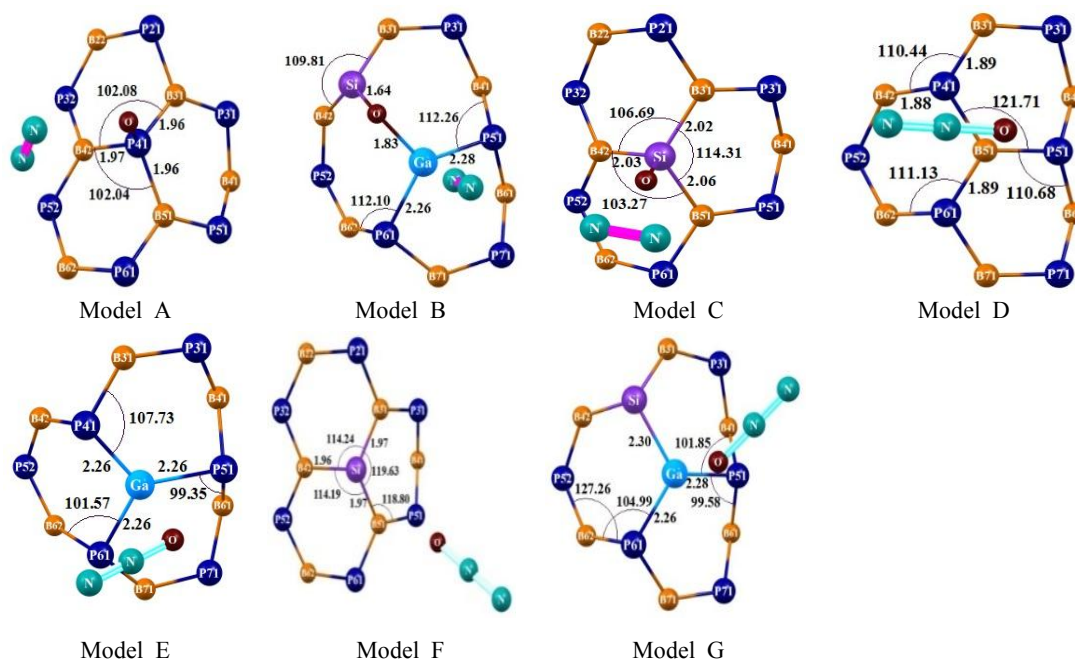


Figure 2. 2-D views of bond length and bond angle of around N₂O adsorption and doping position of (A–G) models (see figure 1).

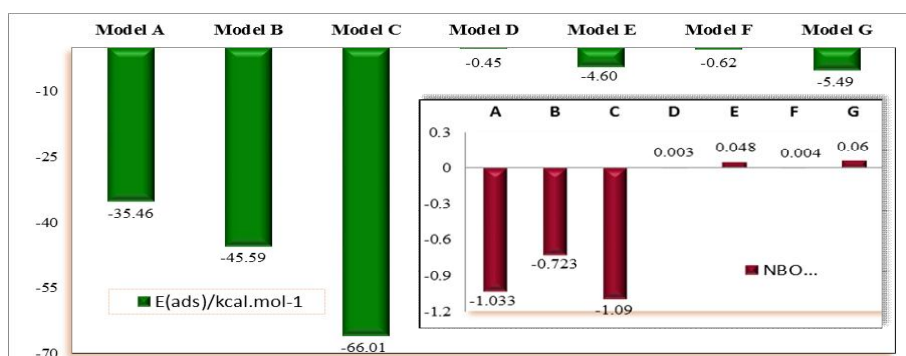


Figure 3. Plots of N₂O adsorption energy and $\Delta\rho$ NBO charge transfer of (A–G) models (see figure 1).

slightly from those of pristine models. Moreover, with doping Ga on B51 nuclei, the average bond length increases significantly from 1.89 to 2.25 Å and the bond angle decreases significantly from 121.40° to 107.67°. When Si and Ga atoms are doped together on P41 nuclei and B51 nuclei, the average bond length increases significantly from 1.89 to 2.29 Å and the bond angle decreases significantly from 121.77° to 113.67°. The radius of Ga atom is larger than that of B atom, and so Ga doping in nanotube distributes the charge electron density around doping position and so the bond length and bond angle of Ga-doped model change considerably compared to the pristine model.

To study the adsorption of N₂O gas on the surface of BPNTs, the interaction of N₂O gas with O-site on the surface of nanotube has been investigated. Since oxygen atom is more electronegative than nitrogen atom for configuration, in which oxygen atom orients toward BPNTs surfaces, the interaction between N₂O gas and surfaces of nanotube is more than other orientations. For this reason, two different configurations have been considered for adsorption of N₂O gas on the surface of nanotube: (1) adsorption of N₂O gas on the nonmetal site of nanotube (A–C models, figure 1), (2) adsorption of

N₂O gas on the metal site of nanotube (D–G models, figure 1).

The optimized configurations of N₂O adsorption on the surface of BPNTs in figure 1 show that, when N₂O gas localizes on the metal site, N₂O gas is gradually bent inward, away from B atom and adsorption of N₂O is in molecule form on the horizontal surface of nanotube. Therefore, the bond length (B–P) and bond angle (B–P–B) of (D–G) models, change slightly from original values (due to physisorption of N₂O (figure 2). When N₂O gas localizes on the nonmetal site, it is dissociated to O atom, which is adsorbed on nonmetal nuclei; and N₂ molecule which is formed on the parallel surface of nanotube.

Therefore, bond length (B–P) around the adsorption position in (A–C) models increases slightly from pure models and bond angle (B–P–B) decreases significantly from those of pure models (figure 2).

Adsorption energy (E_{ads}) of A–G models is calculated by using eqs.1 and the results are given in Appendix (table 2) and are shown in figure 3. The results of figure 3 indicate that adsorption energy of all models is negative and all adsorption processes are exothermic in thermodynamic approach. The results show that

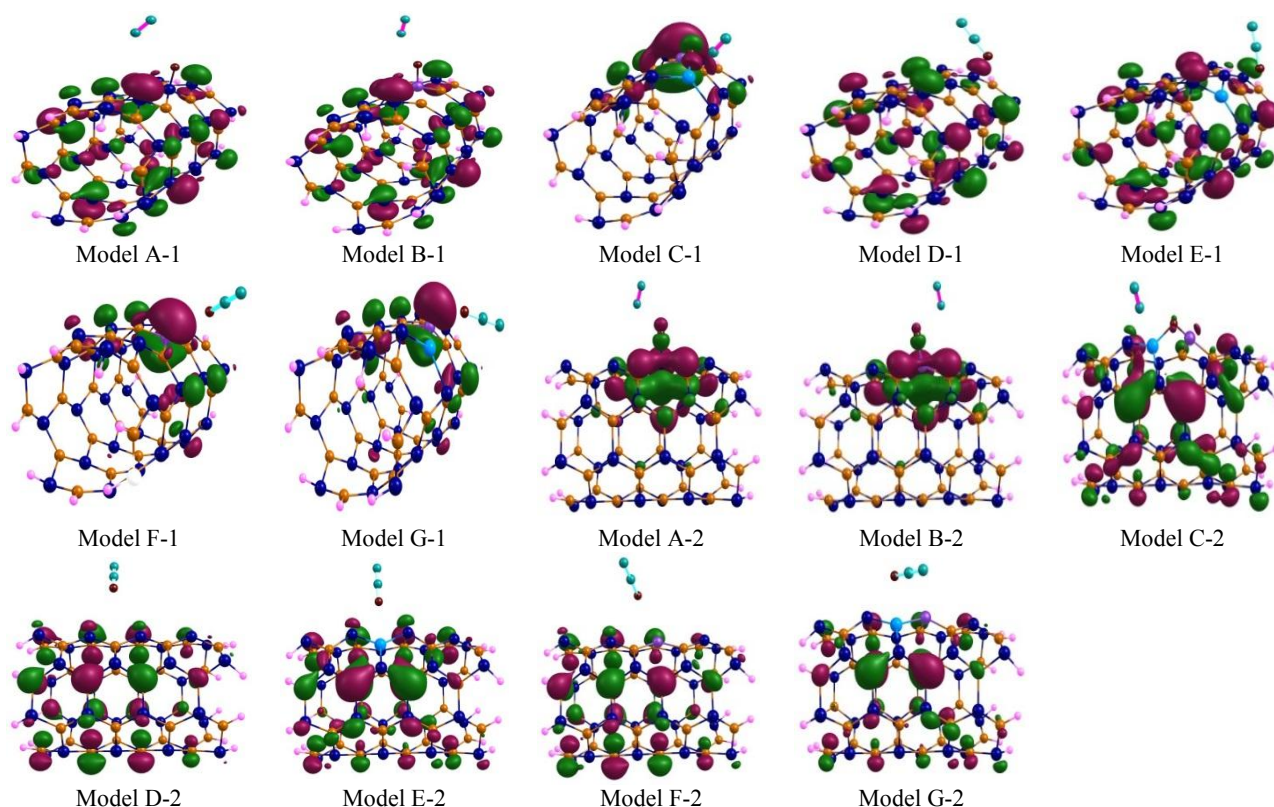


Figure 4. HOMO-LUMO structures of N_2O adsorption on the surface of (4, 4) armchair model of BPNTs (A-G) models, index (1) used for HOMO and index (2) for LUMO (figure 1).

adsorption of N_2O gas at A–C models is in chemisorption form due to dissociation of O atom from N_2O gas and strong adsorption of O atom on the surface of nanotube. Therefore, adsorption energy of A–C models is in the range of -35.46 to -66.01 Kcal/mol and is more than those of the other models. On the other hand, low energy gain from adsorption of N_2O gas at D–G models is in the range of -0.45 to -5.49 Kcal/mol indicating that the chemical interaction between N_2O gas and BPNTs is weak and its bond character is physisorption (figure 3).

The results show that adsorption energy of C model is more than those of other models and adsorption energy of D model is lower than those of other models. It is notable that in the pristine model of BPNTs, adsorption of N_2O gas on the P site of nanotube (A model) is more favorable than B site of nanotube (D model). The comparison results indicate that doping of Si, Ga and GaSi increase the adsorption of N_2O gas on the surface of nanotube. The effect of GaSi dopant on the adsorption of N_2O gas is more than Ga and Si dopants and so C model is the most stable configuration.

3. 2. Quantum molecular descriptors

To further study the adsorption properties of N_2O gas on the surface of pristine, Ga-, Si- and GaSi-doped boron phosphide nanotube, the Highest Occupied Molecular Orbital (HOMO) and the Lowest Unoccupied Molecular Orbital (LUMO) have been investigated. HOMO and LUMO structures are calculated by DFT method and are shown in figure 4. The comparison results of figure 4 reveal that, HOMO orbitals of A, B, D and E models and LUMO orbitals of C, D, E, F and G models are distributed

uniformly throughout the center of nanotube axis, which illustrates that covalent functionalization is preferable throughout the nanotubes. On the other hand, HOMO orbitals of C, F and G models and LUMO orbitals of A and B models distribute around adsorption position. The results reveal that in all the models, HOMO orbitals are localized on the nitrogen atoms and LUMO is more localized on B–P bonds at the center of nanotube.

From E_{HOMO} and E_{LUMO} energies, quantum molecular descriptor parameters including Fermi level energy (E_{FL}), chemical potential (μ), global hardness (η), electrophilicity index (ω), energy gap (ΔE_{gap}), global softness (S), electronegativity (χ) and work function (ϕ) of nanotubes are calculated by eqs. (2–9) and the results are given in Appendix (table 2) and figures (5–7). Inspection of the calculated results indicate that, with adsorption of N_2O gas on pristine, Si, Ga and GaSi-doped BPNTs surface, E_{HOMO} and E_{LUMO} energies for A–E models are decreased from pure nanotube, therefore both groups of occupied and unoccupied molecular orbital are more stable than BPNTs. Furthermore, E_{HOMO} and E_{LUMO} energies for F and G models are increased slightly from pure nanotube.

Fermi level energy is the total chemical (or electrochemical) potential for electrons and is used to determine the thermodynamic work required to add one electron to the system (not counting the work required to remove the electron from wherever it came). A precise understanding of Fermi energy level can relate electronic band structure with electronic properties of nanotube. figure 5 reveals that Fermi level energy of all the models is toward E_{HOMO} and is in the range of -4.234 to -6.169

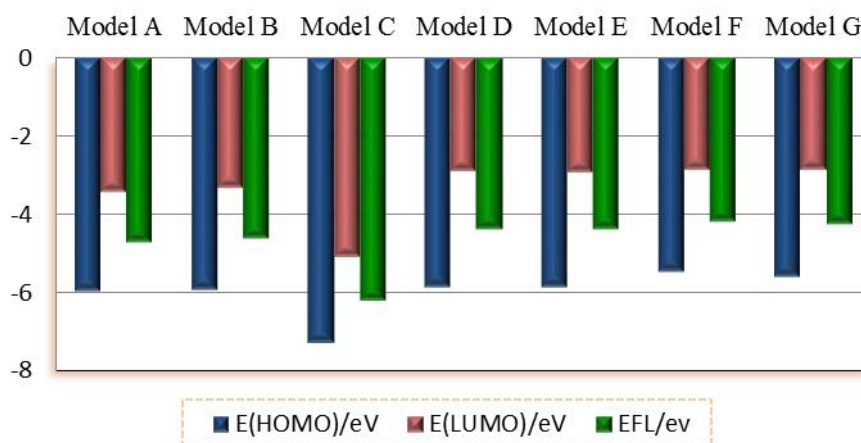


Figure 5. Plots of HOMO, LUMO and Fermi level energy of (A–G) models (figure 1).

eV. The comparison results show that Fermi level energy of C model is larger than other models and that of G model is lower than those of other models. The location of Fermi level energy relative to E_{HOMO} is probably the most important factor in determining the current, and understanding it assists in determining the direction of natural flow of electrons where the two materials are joined. Therefore, knowing this has significant practical applications.

Energy gap (E_{gap}) is a significant parameter which is used to determine the chemical activity and semi-conductivity of the nanotube. A small value for energy gap means a high chemical activity and semi-conductivity of the nanotube. The calculated energy gap of unadsorbed and adsorbed models of BPNTs are given in Appendix (table 2) and shown in figure 7. The comparison results show that energy gap for pristine, Si, Ga, SiGa-doped of unadsorbed BPNTs is in the range of 2.610 to 2.963 eV. The results show that the energy gap of Si doped is lower than pristine, and so the chemical activity of Si-doped BPNTs is higher than other pristines.

The results indicate that, with doping Si, Ga and SiGa, gap energy reduces slightly from pristine models and so their electrical conductance of doped models increases from pristine model. When N₂O gas is adsorbed on the surface of BPNTs in A, B and C models, the energy gap reduces from original values, thus, the chemical activity of these models will be slightly increased, and in other models, the energy gap is slightly constant.

One of the important physical properties of nanomaterials in solid state is the Density of State (DOS) spectrum. DOS spectrum of a system describes the number of states per interval of energy at each energy level that are available to be occupied. A high DOS at a specific energy level means that there are many states available for occupation. In this work by using GaussSum program [30], DOS of spectrum has been obtained from the output of HOMO and LUMO calculations for BPNTs before and after N₂O adsorption and is shown in figure 6.

The results of figure 6 reveal that DOS spectrum in pure BPNTs has six peaks in HOMO region and four

peaks in LUMO region in the energy range of –10 to 0 eV. In Si, and SiGa-doped BPNTs, it is found that DOS spectrum is split to alpha and beta spectra and also in the range of –5.8 and –4 eV, two small peaks are shown. But in Ga-doped BPNTs, DOS spectrum is similar to pristine form and Ga doping slightly reduces the energy gap and height peak in the LUMO region. It can be seen that DOS spectrum of N₂O adsorption on the surface of pristine, Si-, Ga-, and SiGa-doped BPNTs displays more reasonable changes than DOS of the pure BPNTs, revealing the slight effect of N₂O gas on the electronic conductivity of BPNTs. The results exhibit that the slight difference of DOS spectrum is between A–G models and A–D models. These results show that after the adsorption of N₂O on the surface of BPNTs (A–G models), the HOMO–LUMO energy gap of nanotubes has a notable alter. This is an evidence of the interaction between N₂O and BPNTs. Comparison of DOS spectrum before and after adsorption of N₂O shows that the height of all DOS peaks in HOMO and LUMO region of N₂O adsorption reduced slightly from pure nanotubes. In addition, the number of DOS peaks of A–C models is lower than A–C pure models, due to chemical adsorption of N₂O gas on the surface of BPNTs and dissociation of O atom from N₂O. On the other hand, the number of DOS peaks in D–G models before and after N₂O adsorption is constant and the height of all DOS peaks changes slightly. This result demonstrates that the chemical adsorptions of N₂O gas changes the electrical properties of nanotube significantly and the variation of these properties is useful in industrial applications.

To better understand the nature of interaction between N₂O and BPNTs, the influence of N₂O adsorptions on other quantum properties have been studied here involving: chemical potential (μ), global hardness (η), electrophilicity index (ω), electronegativity (χ) and work function (ϕ). The calculated results are given in Appendix (table 2) and shown in figure 7. The calculated results show that the global hardness (η) of pure BPNTs is 1.482 eV and with doping Si, Ga and SiGa decrease to 1.305, 1.456 and 1.362, respectively. Decreasing global hardness leads to decrease in stability and increase in reactivity of the species. When N₂O gas is adsorbed on the surface of BPNTs in A, B and C

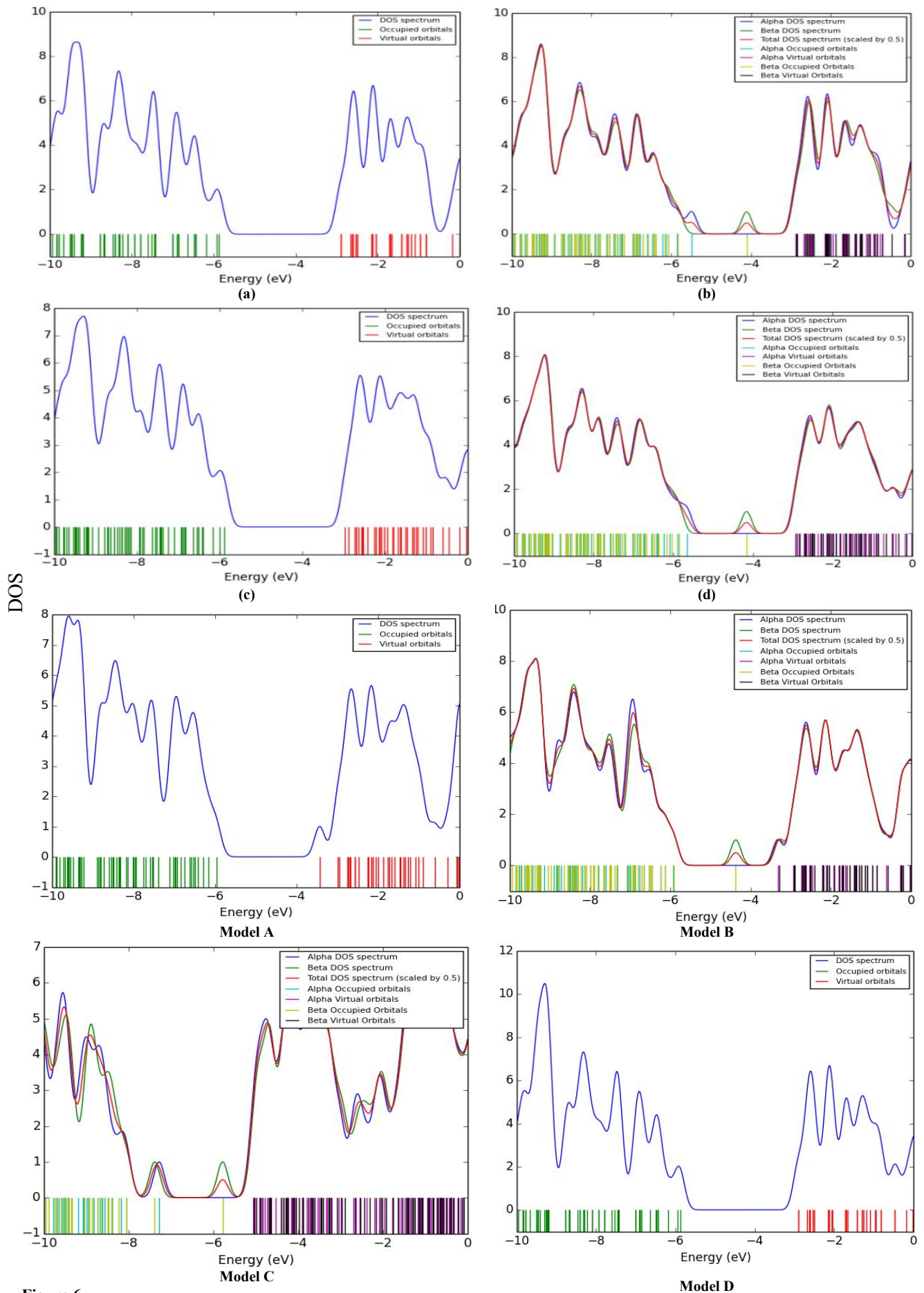


Figure 6.

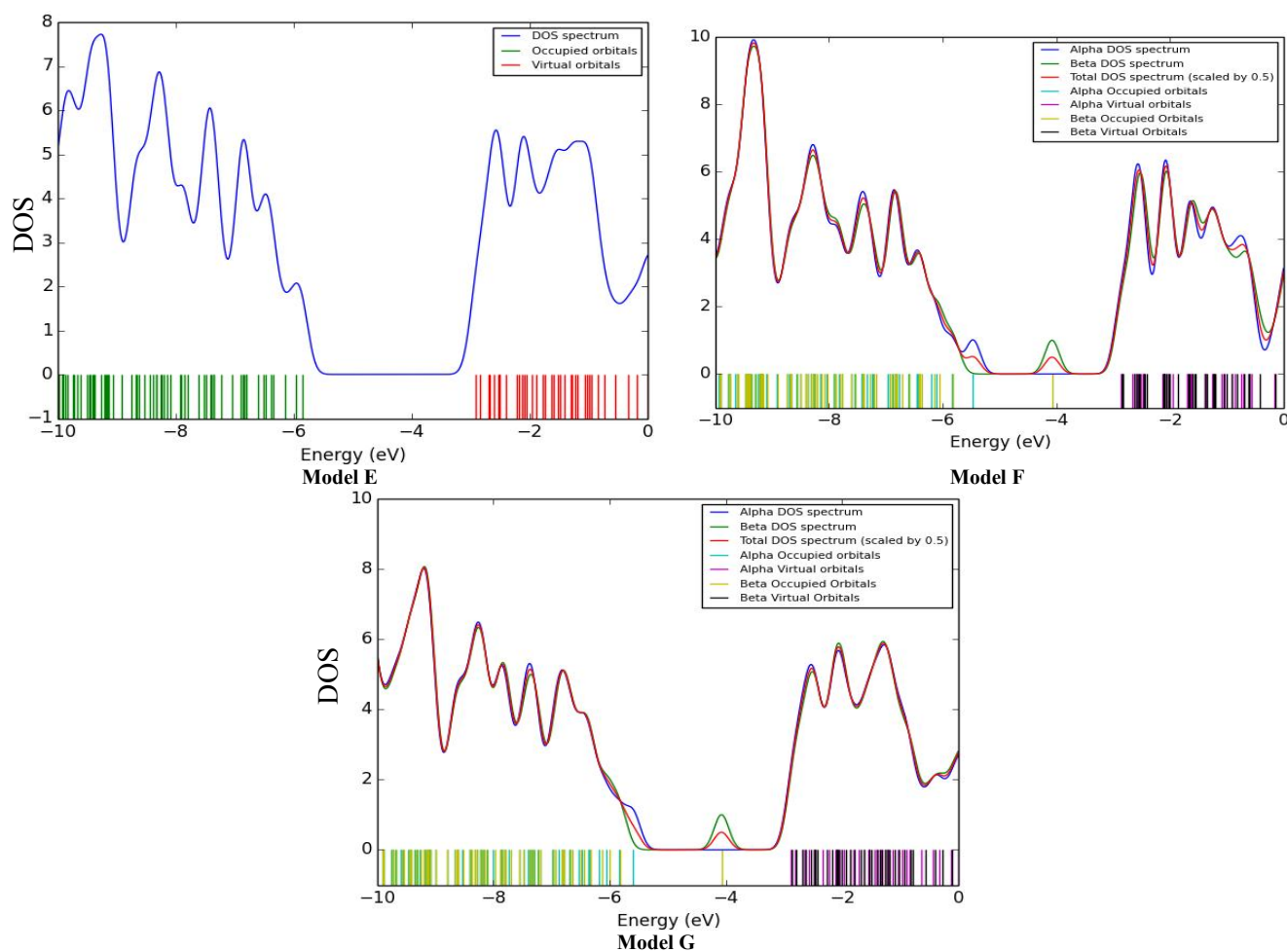


Figure 6. Plots of density of state (DOS) spectrum of (A-G) models (figure 1).

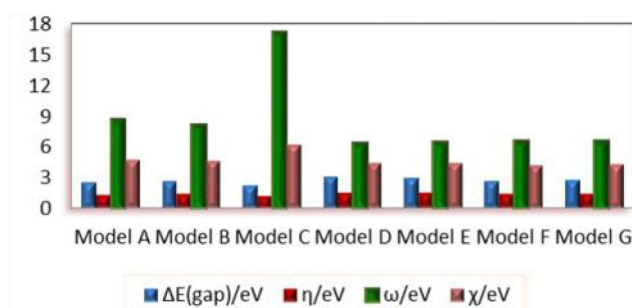


Figure 7. Plots of energy gap (E_{gap}), global hardness (η), electrophilicity index (ω), and electronegativity (χ) of (A-G) models (figure 1).

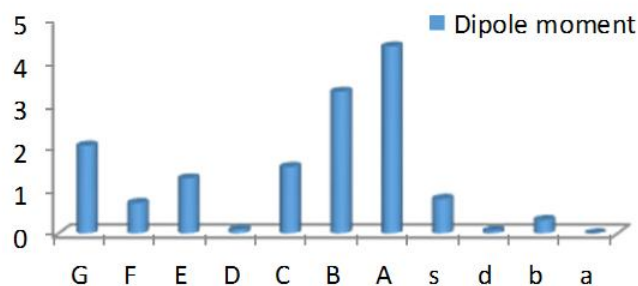


Figure 8. Plots of dipole moment of the unabsorbed N₂O (models A, B, C, and D) and (A-G) models (figure 1).

models, the global hardness decreases significantly from pure values. On the other hand, the electrophilicity index (ω), electronic chemical potential (μ), electronegativity

(χ) and global softness (S) of A, B and C models increase significantly from pure BPNTs. Therefore, the comparison results confirm that chemical adsorption of

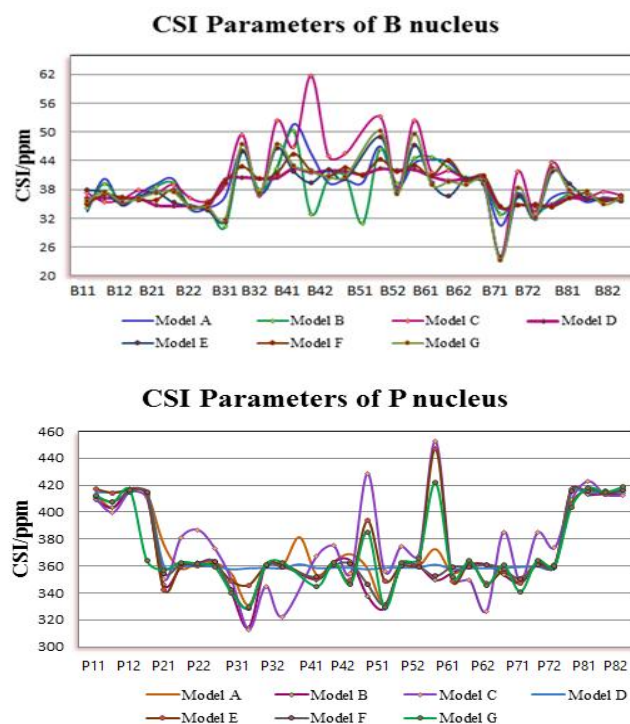


Figure 9. CSI parameters of B and P nuclei of (A–G) models.

N₂O gas on the surface of BPNTs decreases the stability of nanotube and increases the reactivity of nanotubes. Increasing electronic chemical potentials and electronegativity of nanotube reveal that a slight charge transfer to the nanotube could occur and their electronic transport properties could be slightly changed upon adsorptions of N₂O. In thermodynamic approach, the direction of charge transfer is from higher chemical potential to lower electronic chemical potential, until the electronic chemical potentials become identical. Therefore, the comparison results of electronic chemical potentials and electronegativity of A–C models clarify that the charge transfer occurs from a definite occupied orbital in an O atom of N₂O gas to a definite empty orbital in BPNTs. On the other hand, the electrophilicity index determines the maximum flow of electron from donor to acceptor species and supplies data connected to structural stability, reactivity and toxicity of chemical species.

The work function is a minimum energy needed to remove an electron from a solid to a point in the vacuum immediately outside the solid surface. The calculated results describe that the work function (ϕ) of A–C models decreases significantly from pure nanotube. According to Richardson's law the emitted current density (per unit area of emitter), J_e (A/m²), is related to the absolute temperature T_e of the emitter by the following equation:

$$J_e = AT^2 e^{-\phi/KT}, \quad (12)$$

where (A) is Richardson type constant. With decreasing work function, the emitted current density of nanotube decreases. Among theoretical methods, NBO analysis [31] is a unique approach to evaluate the atomic and molecular charges. To study the charge transfer between N₂O gas and nanotube, the charge concentration ($\Delta\rho$) is

calculated from the difference between N₂O gas after adsorption and an isolated N₂O. The calculated NBO results are given in figure 3. The negative values of $\Delta\rho$ for A, B and C models demonstrate that N₂O gas is an acceptor of electron species. The $\Delta\rho$ values for other models are positive, among all the models, C and D models have the largest and smallest amount of charge transfer respectively. According to obtained results, (figures 3 and 7), the trend of adsorption energy, the electrophilicity index (ω) and NBO charge in all the models are similar. In C model, the values of NBO charge, adsorption energy, and the electrophilicity index are larger than those of other models.

On the other hand, when N₂O gas is adsorbed on the surface of BPNTs the dipole moment of nanotube changes significantly from unabsorbed nanotube forms. From inspection of the results of figure 8, it can be observed that the dipole moment of A and B models are larger than those of other models. It is notable that doping a foreign impurity and adsorbed N₂O gas causes the dipole moment of nanotube to change significantly from pristine models, due to charge electrons distribution of nanotube and it is important for detecting electrical properties of nanotube.

3.3 NMR parameters of N₂O adsorption on BPNTs

NMR parameters of ¹¹B and ³¹P sites for adsorption of N₂O gas on the surface of pristine, Si-, Ga- and SiGa-doped of BPNTs A–G models are summarized in Appendix (tables 3,4) and the plots of CSI parameters are shown in figure 9. In our previous work [21–24], it was shown that in pristine model of BPNTs, NMR parameters were separated into four layers, which means that CS parameters for the atoms of each layer have equivalent chemical environments and electrostatic

properties. When N₂O gas is adsorbed on the surface of BPNTs, the CSI values in A–B models change significantly from pure nanotube, due to chemical adsorption of N₂O gas and dissociation of O from N₂O molecule. On the other hand, the CSI values of D–G models change slightly from original values due to physical adsorption of N₂O gas. NMR parameters of various B atoms in Ga, and SiGa-doped BPNTs show some significant changes in boron nuclei directly bonded to Ga atom. Hence, both the CSI and CSA parameters show important changes due to Ga, and SiGa doping. Among P atoms of BPNTs, in comparison with pristine model, the greatest changes in NMR parameters are observed for P41, P51, P61 atoms, and both CSI and CSA parameters show significant changes which are due to the substitution of Ga atoms. The CSI values of B52 site of Si doped models increase significantly from original values. On the other hand, the CSI values of the B71 site decrease significantly from original values. According to the calculated results, as shown in figures 9 and 10, the CSI values for B nuclei on B32, B42, B52 and B62 atoms of A, C, D, E, F and G models are larger than those of other atoms. The comparison results show that the CSI values at B42 atoms of C model are larger than those of other models. Moreover, the CSI values of B model at B42 and B52 atoms are lower than those of other models.

The CSI values of P22, P51, and P61 atoms of A, B, D, E, F and G models are larger than those of other atoms. The CSI trend of P22, P51 and P61 nuclei for B, C and G models is: C model > B model > G model. These results confirm that, the adsorption of N₂O gas increases the density of electron on P atoms around adsorption position. This trend is in agreement with the change in the gap energy of adsorption models in comparison with pure BPNTs. Increasing CSI values decreases gap energy and increases the activity of

nanotube.

4. Conclusions

In this project, the interaction of N₂O gas on the surface of pristine, Ga-, Si- and SiGa- doped on (4,4) armchair models of BPNTs is investigated by using density functional theory. For this purpose, adsorption of N₂O gas from O head on B and P atoms of nanotube has been investigated. Comparison of results showed that when N₂O gas is adsorbed on the nonmetal position of nanotube, N₂O gas was dissociated to O atom and N₂ molecule. The O atom strongly is adsorbed atop surface of nanotube, the electrical and structural parameters of nanotube changed significantly from original values. On the other hand, gap energy, global hardness, electrophilicity index and other quantum parameters changed significantly. With adsorbing N₂O gas on the B site of nanotube (D–G models) the electrical and structural parameters changed slightly from original values. Adsorption energy values of all the models were negative and all processes were exothermic according to thermodynamic approach. Adsorption energy of C model was more than that of other models and this model was more stable than other models. When N₂O gas is adsorbed atop surface of BPNTs in A, B and C models, global hardness decreased significantly from pure values. On the other hand, electrophilicity index (ω), electronic chemical potential (μ), electronegativity (χ) and global softness (S) of A, B and C models increased significantly from pure BPNTs. The results revealed that CSI values of P22, P51 and P61 nuclei for B, C and G model were: C model > B model > G model.

Acknowledgment

The authors thank the Centre of computational nano of Malayer University for supporting this research.

References

1. A S Tarendash, "Let's Review: Chemistry, the Physical Setting", Barron's Educational Series (2004).
2. M Iwamoto and H Hamada, *Catal. Today* **10** (1991) 57.
3. F Kaptein, J Rodriguez-Mirasol, and J A Moulijn, *App. Catal. B* **9** (1996) 25.
4. G Delahay, M Mauvezin, B Coq, and S Kieger, *J Catal.* **202** (2001) 156.
5. B Coq, M Mauvezin, G Delahay, J B Butet, and S Kieger, *App. Catal. B* **27** (2000) 193.
6. B Moden, P Da Costa, B Fonfe, D Ki Lee, and E Iglesia, *J. Catal.* **209** (2002) 75.
7. A Martinez, A Goursot, B Coq, and G Delahay, *J. Phys. Chem. B* **108** (2004) 8823.
8. A R Ravishankara, J S Daniel, and R W Portmann, *Science* **326** (2009) 23.
9. M T Baei, A Soltani, A V Moradi, and E Tazikeh Lemeski, *Com. Theo. Chem.* **970** (2011) 30.
10. M T Baei, A Soltani, A V Moradi, and M Moghimi, *Monatsh. Chem.* **142** (2011) 573.
11. A Soltani, M Ramezani Taghartapeh, E Tazikeh Lemeski, M Abroudi, and H Mig, *Superlattice Microst.* **58** (2013) 178.
12. X Solans-Monfort, M Sodupe, and V Branchadell, *Chem. Phys. Lett.* **368** (2003) 42.
13. M Mirzaei, *Z Phys. Chem.* **223** (2005) 815.
14. M T Baei, A Varasteh Moradi, P Torabi, and M Moghimi, *Monatsh. Chem.* **142** (2011) 1097.
15. M T Baei, A Ahmadi Peyghan, and M Moghimi, *Monatsh. Chem.* **143** (2012) 1627.
16. M T Baei, *Monatsh. Chem.* **143** (2012) 881.
17. M Mirzaei, *J. Mol. Model* **17** (2011) 89.
18. A Ahmadi Peyghan M T, Baei, M Moghimi, and S Hashemian, *J. Clust. Sci.* **24** (2013) 49.
19. M T Baei, A Varasteh Moradi, P Torabi, and M Moghimi, *Monatsh. Chem.* **143** (2012) 37.
20. K Li, W Wang, and D Cao, *Sensor Actuat. B Chem.* **159** (2011) 171.
21. M Rezaei-Sameti, *Physica B* **407** (2012) 3717.
22. M Rezaei-Sameti, *Physica E* **44** (2012) 1770.
23. M Rezaei-Sameti, and S Yaghoobi, *Comp. Condense*

- Matt.* **3** (2015) 21.
 24. M Rezaei-Sameti, *Physica B* **407** (2012) 22.
 25. M Rezaei-Sameti, and E A Dadfar, *Iranian J. Phys. Res.* **15** (2015) 41.
 26. M J Frisch, et al., Gaussian 03, Inc., Pittsburgh (2003).
 27. P K Chattaraj, U Sarkar, and D R Roy, *Chem. Rev.* **106** (2006) 2065.
 28. K K Hazarika, N C Baruah, and R C Deka, *Struct. Chem.* **20** (2009) 1079.
 29. R G Parr, L Szentpaly, and S Liu, *J. Am. Chem. Soc.* **121**(1999) 1922.
 30. C Tabtimisai, S Keawwangchai, N Nunthaboot, V Ruangpornvisuti, and B Wann, *J. Mol. Model.* **18** (2012) 3941.
 31. A E Reed, L A Curtiss, and F Weinhold, *Chem. Rev.* **88** (1988) 899.

Appendix

Table 1. Structural parameters of adsorption N₂O molecule on the surface pristine and Si, Ga, SiGa doped of BPNTs models (A-G in figure 1).

Bond length(Å)	Pristine	Ga-doped	Si-doped	GaSi-doped	Model A	Model B	Model C	Model D	Model E	Model F	Model G
B31-P41/Si	1.97	1.89	1.88	1.88	1.96	2.02	1.97	1.89	1.92	1.97	1.97
P52-B42	1.97	1.92	1.91	1.94	1.89	1.86	1.89	1.89	1.91	1.88	1.89
B42-P41/Si	1.88	1.92	1.91	1.93	1.97	2.03	1.96	1.88	1.91	1.96	1.97
P41/Si-B51/Ga	1.92	2.26	1.87	2.27	1.96	2.06	2.24	1.90	2.26	1.97	2.30
B51/Ga-P61	1.90	2.25	1.97	2.29	1.90	1.89	2.26	1.89	2.26	1.88	2.26
P51-B51/Ga	1.89	2.25	1.88	2.25	1.86	1.86	2.28	1.88	2.26	1.88	2.28
Bond Angle(°)											
B31-P41/Si-B42	120.73	98.49	111.22	100.10	102.08	106.69	109.81	110.44	105.38	114.24	112.26
B31-P41/Si-B51/Ga	121.67	122.83	118.66	119.46	118.24	114.31	111.10	116.69	107.73	119.63	113.91
B42-P41/Si-B51/Ga	121.77	107.67	119.70	113.01	102.04	103.27	110.80	110.63	101.42	114.19	108.50
P41/Si-B42-P32	121.38	125.25	117.97	121.15	120.58	118.08	110.90	121.76	117.47	119.26	115.63
P41/Si-B51/Ga-P61	120.76	100.08	114.23	107.18	114.40	115.38	114.02	116.43	113.25	117.30	115.28
B51/Ga-P61-B62	120.55	113.13	117.41	115.38	106.38	108.94	112.10	111.13	101.57	112.31	104.95

Table 2. Quantum parameters of N₂O adsorption on the surface of (4,4) armchair BPNTs (models A – G in figure 1).

Property	Pristine	Si-doped	Ga-doped	GaSi-doped	Model A	Model B	Model C	Model D	Model E	Model F	Model G
E _{ads} /kcal mol ⁻¹	-	-	-	-	-35.459	-45.589	-66.005	-0.449	-4.602	-0.617	-5.488
E _{HOMO} /eV	-5.864	-5.489	-5.878	-5.649	-5.967	-5.918	-7.282	-5.867	-5.850	-5.461	-5.592
E _{LUMO} /eV	-2.901	-2.925	-2.966	-2.925	-3.431	-3.320	-5.056	-2.903	-2.917	-2.865	-2.876
E _{gap} /eV	2.963	2.610	2.912	2.724	2.536	2.599	2.226	2.963	2.933	2.596	2.716
I/eV	5.864	5.489	5.878	5.649	5.967	5.918	7.282	5.867	5.850	5.461	5.592
A/eV	2.901	2.879	2.966	2.925	3.431	3.320	5.056	2.903	2.917	2.865	2.876
η/eV	1.482	1.305	1.456	1.362	1.268	1.299	1.113	1.482	1.467	1.298	1.358
μ/eV	-4.382	-4.184	-4.422	-4.287	-4.699	-4.619	-6.169	-4.385	-4.384	-4.163	-4.234
S/eV	0.337	0.383	0.343	0.367	0.394	0.385	0.449	0.337	0.341	0.385	0.368
ω/eV	6.481	6.708	6.715	6.748	8.708	8.210	17.096	6.489	6.551	6.677	6.601
χ/eV	4.382	4.184	4.422	4.287	4.699	4.619	6.169	4.385	4.384	4.163	4.234
E _{FL} /ev	-4.382	-4.184	-4.422	-4.287	-4.699	-4.619	-6.169	-4.385	-4.384	-4.163	-4.234
φ/eV	-1.482	-1.305	-1.450	-1.362	-1.268	-1.299	-1.113	-1.482	-1.467	-1.298	-1.358
Δρ(NBO)	-	-	-	-	-1.033	-0.723	-1.090	0.003	0.048	0.004	0.060
Dipole moment	0.002	0.317	0.065	0.812	4.385	3.324	1.561	0.095	1.291	0.714	2.061

Table 3. NMR parameters for adsorption of N₂O on the surface of (4, 4) armchair BPNTs (models A – C in figure 1).

<i>Nuclei</i>	CSI			CSA		
	Model A	Model B	Model C	Model A	Model B	Model C
P11	413	410	410	117	117	124
P12	403	404	400	92	103	118
P21	376	346	350	223	215	170
P22	358	358	381	215	221	176
P31	354	340	349	160	169	131
P32	331	315	313	126	105	204
P41/Si	381	338	280	239	27	52
P42	354	349	367	217	228	212
P51	358	338	429	164	189	70
P52	331	329	356	142	122	168
P61	373	348	453	216	223	108
P62	355	355	351	223	227	211
P71	355	354	385	173	163	104
P72	352	348	349	116	116	151
P81	417	418	409	107	115	68
P82	413	414	423	109	113	114
B11	33	34	37	103	95	144
B12	40	39	35	101	103	134
B21	39	39	37	114	116	53
B22	40	39	39	90	98	36
B31	36	30	39	77	90	128
B32	46	46	49	80	82	118
B41	52	50	47	92	86	33
B42	46	33	62	88	75	76
B51/Ga	39	31	-	80	58	192
B52	47	46	53	78	85	122
B61	44	45	42	91	87	28
B62	44	43	42	73	70	68
B71	30	33	24	64	70	109
B72	37	36	42	66	70	123
B81	37	37	38	105	100	51
B82	35	36	36	92	99	58

Table 4 NMR parameters for adsorption of N₂O on the surface of (4,4) armchair BPNTs (models D – G in figure 1).

<i>Nuclei</i>	CSI				CSA			
	Model D	Model E	Model F	Model G	Model D	Model E	Model F	Model G
P11	415	417	411	413	92	85	96	90
P12	415	414	408	407	57	74	90	98
P21	360	343	355	357	245	242	227	206
P22	360	360	362	363	245	242	224	215
P31	358	349	342	340	89	107	180	155
P32	358	346	329	329	88	128	186	207
P41/Si	361	446	270	236	246	225	158	99
P42	358	350	352	345	249	253	241	245
P51	358	394	346	385	103	144	179	77
P52	359	349	331	329	101	111	183	216
P61	361	447	352	422	237	202	215	209
P62	358	349	360	352	241	247	219	228
P71	359	356	358	360	86	103	152	163
P72	359	347	350	341	82	112	153	174
P81	415	406	416	404	115	97	114	92
P82	414	417	416	418	120	123	124	121
B11	36	38	35	36	141	146	133	123
B12	36	37	37	38	120	127	122	123
B21	35	37	36	37	83	72	33	36
B22	35	35	38	37	83	54	28	24
B31	40	31	40	32	99	103	129	125
B32	40	46	43	47	99	105	108	109
B41	42	42	45	43	66	55	42	31
B42	42	39	42	42	66	34	55	83
B51/Ga	41	-	41	-	103	105	141	363
B52	42	49	44	50	102	111	114	117
B61	41	39	41	39	34	31	32	22
B62	40	37	44	40	57	36	36	64
B71	34	24	34	23	99	99	116	105
B72	35	37	35	38	100	36	122	123
B81	36	39	36	38	69	65	62	59
B82	36	36	37	38	65	41	64	68